Isothermal Chemical Denaturation as a Complementary Tool to Overcome Limitations of Thermal Differential Scanning Fluorimetry in Predicting Physical Stability of Protein Formulations

Hristo Svilenov[1] †, Uroš Markoja[2], Gerhard Winter[1]

[1]Department of Pharmacy, Pharmaceutical Technology and Biopharmaceutics, Ludwig-Maximilians-University, Butenandtstrasse 5-13, Munich D-81377, Germany

[2]University of Ljubljana, Faculty of Pharmacy, Aškerčeva 7, 1000 Ljubljana, Slovenia

†Corresponding author: hrisph@cup.uni-muenchen.de

Accepted manuscript published with Gold Open Access as:

Svilenov, H., Markoja, U. and Winter, G., 2018. Isothermal chemical denaturation as a complementary tool to overcome limitations of thermal differential scanning fluorimetry in predicting physical stability of protein formulations. European Journal of Pharmaceutics and Biopharmaceutics, 125, pp.106-113.

https://doi.org/10.1016/j.ejpb.2018.01.004

https://doi.org/10.1016/j.ejpb.2018.01.004

ABSTRACT

Various stability indicating techniques find application in the early stage development of novel therapeutic protein candidates. Some of these techniques are used to select formulation conditions that provide high protein physical stability. Such an approach is highly dependent on the reliability of the stability indicating technique used. In this work, we present a formulation case study where we evaluate the ability of differential scanning fluorimetry (DSF) and isothermal chemical denaturation (ICD) to predict the physical stability of a model monoclonal antibody during accelerated stability studies. First, we show that thermal denaturation technique like DSF can provide misleading physical stability ranking due to buffer specific pH shifts during heating. Next, we demonstrate how isothermal chemical denaturation can be used to tackle the above-mentioned challenge. Subsequently, we show that the concentration dependence of the Gibbs energy of unfolding determined by ICD provides better predictions for the protein physical stability in comparison to the often-used T_m (melting temperature of the protein determined with DSF) and C_m (concentration of denaturant needed to unfold 50 % of the protein determined with ICD). Finally, we give a suggestion for a rational approach which includes a combination of DSF and ICD to obtain accurate and reliable protein physical stability ranking in different formulations.

https://doi.org/10.1016/j.ejpb.2018.01.004

Keywords

protein formulation; thermal denaturation; isothermal chemical denaturation; monoclonal antibody; differential scanning fluorimetry;

Abbreviations

µDSC – differential scanning microcalorimetry

C_m – concentration (in M) of chemical denaturant needed to unfold 50 % of the protein ("melting" concentration of denaturant)

dG – Gibbs free energy of unfolding

$dH_{ionisation}$ – enthalpy of ionisation

dpH/dT – temperature dependence of pH in pH units per 1 °C

dpKa/dT – temperature dependence of pKa in pH units per 1 °C

DSF- differential scanning fluorimetry

HMW – high molecular weight species

HP-SEC – size exclusion chromatography

HPW – highly purified water

ICD – isothermal chemical denaturation

ICH – international conference on harmonization

LMW – low molecular weight species

MWCO – molecular weight cut off

pKa – acid dissociation constant

T_m – protein melting temperature

https://doi.org/10.1016/j.ejpb.2018.01.004

1. Introduction

1.1. Therapeutic protein development and formulation

Therapeutic proteins have been largely successful in the treatment of various severe diseases [1–3]. This success led to the development and market approval of many new biologics over the past two decades. Nowadays, almost every big pharmaceutical company has therapeutic proteins in its R&D program [4]. However, the development process of biologics is often more complicated in comparison to small molecules. Proteins can exhibit various degradation pathways which are intrinsic to their complex structure. One such degradation pathway, which is a major quality and safety issue, is the formation of soluble aggregates. It has been demonstrated that the presence of soluble aggregates can result in reduced activity [5,6] and/or trigger immune response followed by the production of anti-drug antibodies [7–9]. Even if immunogenicity is not an issue for a given protein, aggregates fall under the category of product-related impurities according to the ICH guidelines [10] and it is expected that during the shelf life aggregate levels remain within an acceptable range set on a case-by-case study.

Aggregate formation can be reduced by selection of optimal formulation conditions for a new therapeutic protein candidate. Such selection could be based on forced degradation studies followed by accelerated stability testing [11]. However, such studies require a lot of time and a large sample amount (both of which are scarce in the early development stage). For this reason, various high throughput biophysical methods became widespread as tools that can quickly provide data on many formulation conditions with minimal sample consumption. Such high throughput methods are usually used to narrow down the number of promising formulations to few that will move on to forced degradation studies and accelerated and/or real-time stability tests [12–17].

1.2. Aspects of protein stability

Protein stability has various aspects (i.e. physical stability, chemical stability), each of which can contribute to the formation of aggregates and/or affect other quality attributes (e.g. biological activity). The connection between protein physical stability and aggregate formation has been described in detail elsewhere [18–20]. However, the reader should be aware that conditions (e.g. pH, ionic strength) that maximize the physical stability of a protein might have a detrimental effect on the protein chemical stability (e.g. oxidation, deamination). Therefore, the most stable protein formulation could be a compromise where both the physical and chemical stability of the protein is not maximal but sufficient to ensure all aspects of product quality during the shelf life. The stabilization of proteins against chemical changes is outside the scope of our work but more information on this topic can be found in the literature [21].

1.3. Thermal denaturation techniques to study protein physical stability

A commonly used technique to screen formulations for protein physical stability is *differential scanning microcalorimetry (μDSC)*. Excellent review on the background and applications of μDSC can be found elsewhere [22]. μDSC has been successfully used to measure the melting temperatures (T_m) of various proteins in different formulation conditions. The rankings based on T_m values are in some cases in good agreement with the outcome of the accelerated stability studies [23–26]. Although μDSC provides stability indicating data much faster than forced degradation studies (or accelerated stability tests), even μDSC devices equipped with an autosampler can measure only several samples over 24 hours and few milligrams of protein are required to screen different formulation conditions.

https://doi.org/10.1016/j.ejpb.2018.01.004

Differential scanning fluorimetry (DSF) is an alternative to µDSC technique which provides physical stability-indicating data based on the protein melting temperatures in different formulations [13]. Hundreds of T_m values per day can be obtained with modern DSF methods with as less as few micrograms protein needed for one measurement. There are two main approaches to perform DSF – the first is based on an increase in (extrinsic) fluorescence intensity of a fluorescent dye that interacts with hydrophobic protein patches exposed during thermal unfolding [27]. The second approach is label-free and measures the intrinsic tryptophan fluorescence that changes during unfolding due to change in the tryptophan environment [28]. Excellent agreement was demonstrated between T_m values measured by µDSC and DSF with extrinsic fluorescent dye [13,14,29,30] or DSF based on intrinsic protein fluorescence [31].

Whether µDSC or DSF will be used during protein formulation screening is still a matter of debate and preferences of the formulation scientist. An advantage of µDSC is that this technique will usually provide a better resolution between protein unfolding transitions in comparison to DSF [29]. In addition, the detection of protein unfolding by µDSC is independent of the number of tryptophan residues in the structure or the interaction of the extrinsic fluorescent probe with the (partially unfolded) protein. The benefits of DSF techniques are mostly related to the lower sample consumption and the higher throughput in comparison to µDSC.

Regardless whether heat capacity (µDSC) or extrinsic/intrinsic fluorescence (DSF) is measured as a physical observable to detect protein unfolding during heating, all thermal denaturation methods suffer from the fact that the temperature is increased far above the actual temperature of sample preparation and storage. This requires long error-prone extrapolations to lower temperatures during the thermodynamic evaluation of the data [32]. Additionally, thermal protein denaturation is usually a non-reversible process which makes the thermodynamic evaluation of such data invalid and physical stability rankings are based only on T_m values which represent only a small part of the protein conformational stability curve against temperature [32]. On the other hand, aggregation of the protein at temperatures around the melting temperature of the protein will also affect the accuracy of the measured T_m values [33]. These, and other challenges to predict protein physical stability from thermal denaturation experiments are extensively discussed in the following papers [32,34].

In addition to the above-mentioned pitfalls of thermal denaturation techniques, it is an often-ignored fact that not only protein properties but also excipient properties can change during heating. A typical example of this is the pKa change of many pharmaceutical excipients during heating [35,36]. This includes two of the most frequently used buffers for protein therapeutics – histidine and tris [37].

1.4. Isothermal chemical denaturation (ICD) as a tool to study protein physical stability in different formulations

Isothermal chemical denaturation (ICD) was recently proposed as an isothermal method to evaluate protein physical stability in different formulations [32]. A typical ICD experiment includes the preparation of protein samples with increasing concentration of a denaturant (usually guanidinium hydrochloride or urea). After sufficient incubation time needed to reach an equilibrium, a physical observable is measured (e.g. intrinsic fluorescence) to detect at which denaturant concentrations the protein is (partially) unfolded. The approaches to evaluate chemical denaturation data are described in detail elsewhere [32,38,39]. Most evaluation methods can extract several stability-indicating parameters from chemical denaturation graphs e.g. the amount of denaturant needed to unfold 50 % of the protein (C_m) (sometimes also referred as the “melting” concentration of denaturant) and the

https://doi.org/10.1016/j.ejpb.2018.01.004

Gibbs free energy of protein unfolding (dG) [40]. A recently proposed approach would also investigate the variation of dG in samples with different protein concentration (in the same formulation conditions) [41]. It should be noted that in this case, the dG measured is an apparent value. It is suggested that lower concentration dependence of dG is an indicator for a lower aggregation propensity [42]. Until now, there is some limited data that parameters (i.e. C_m) obtained with ICD can provide good predictions of the outcome of accelerated stability studies [43]. To best of our knowledge, the concentration dependence of dG is not directly related to the physical stability of a protein in a wide range of conditions during accelerated stability studies. Considering also the high sample consumption and low throughput of ICD, it is still unclear why and how formulation scientists should use ICD to find optimal formulation conditions of a new therapeutic protein candidate in early-stage development.

1.5. Problem statement and hypothesis

The reason we stepped into this work is the trend that high throughput thermal denaturation techniques based on T_m measurements are often used on a wide range of formulations to access protein physical stability.

In addition to this, we hypothesized that such thermal denaturation techniques are not an appropriate choice for all formulations, especially such containing excipients that change their properties upon heating. We expected that such “inappropriate” use of thermal denaturation techniques could result in misleading physical stability rankings and probably early rejection of stable protein formulations.

As identifying the problem is just the first step of the solution, we also wanted to investigate whether isothermal chemical denaturation can find a place as a suitable protein physical stability indicating method in cases where high throughput thermal denaturation might not be an appropriate choice.

To test our hypothesis, we developed a classical formulation case study where we investigated the effect of pH and buffer type on the physical stability a model monoclonal antibody (mAb1). Next, we compared thermal and chemical denaturation to see if both methods provide similar predictions for the different conditions we tested. Finally, we performed accelerated stability studies to validate the predictions obtained by DSF and ICD.

2. Materials and Methods

2.1. Model protein and sample preparation

The model monoclonal antibody (mAb1) used in this work is a humanized IgG type 1 with a molecular weight of 145 kDa. The bulk solution has more than 99,5 % relative monomer content after thawing (measured by size exclusion chromatography - see Section 2.5). Further, SDS-PAGE shows only bands corresponding to the monomer and antibody fragments (this data is available on request). mAb1 was selected as a suitable model protein since it shows T_m dependence versus pH which is well described for other IgG type 1 antibodies [13]. In addition, our experience shows that the rate of aggregation of mAb1 is highly dependent on the buffer it is formulated in. This behaviour makes it a good model protein to compare the prediction quality of stability indicating techniques when it comes to the selection of a buffer in a narrow pH range.

https://doi.org/10.1016/j.ejpb.2018.01.004

Different formulations of mAb1 were prepared by dialysis at room temperature (20 – 25 °C) against an excess of the respective buffer using Spectra/Por® 8000 MWCO dialysis tubing from Spectrum Laboratories Inc. (Rancho Dominguez, USA). Sample to buffer ratio was 1:200 and the buffer was exchanged 3 and 8 hours after the start of the dialysis. The total dialysis time was 24 hours. Protein concentration was measured on Nanodrop 2000 (Thermo Fisher Scientific, Wilmington, USA). Finally, the formulations were sterile filtered with 0.22 µm cellulose acetate filters from VWR International (Darmstadt, Germany). Reagent chemicals were of analytical grade and were purchased from Sigma Aldrich (Steinheim, Germany) or VWR International (Darmstadt, Germany). Highly purified water (HPW, Purelab Plus, USF Elga, Germany) was used for the preparation of all buffers.

2.2. Differential scanning fluorimetry (DSF) with intrinsic fluorescence and static light scattering detection

Thermal denaturation studies were performed with the Optim® 1000 system (Avacta Analytical, United Kingdom). 9 µL of mAb1 formulations with protein concentration 10 g/L were filled in triplicates in micro cuvette arrays (Unchained Labs, USA). The samples were excited at 266 nm and fluorescence spectra were collected from 30 to 90 ^{o}C using a temperature ramp of 1 °C/min. Obtained intrinsic fluorescence spectra were further processed to create graphs of the fluorescence intensity ratio 350 nm/330 nm (F350/330) versus temperature. The T_m values were determined from the maximum of the first derivatives of these graphs using the Optim® 1000 software (Avacta Analytical, United Kingdom). T_m1 was assigned to the first transition (at a lower temperature) while T_m2 was assigned to the second transition (at a higher temperature). Simultaneously with the intrinsic fluorescence, static light scattering data at 473 nm was collected by the instrument to evaluate if the protein was aggregating after unfolding.

2.3. Isothermal chemical denaturation (ICD) with intrinsic fluorescence detection

8 µL from of each stock solution of mAb1 with concentration 5, 10, 20 or 40 g/L were pipetted in triplicates with a 16-channel 12,5 µL Viaflo pipette (Integra Biosciences, Konstanz, Germany) and Viaflo Assist (Integra Biosciences, Konstanz, Germany) into non-binding surface 384 well plates (Corning, USA). Next, the respective amount of the formulation buffer and subsequently the denaturant stock solution (same as the formulation buffer regarding concentration and pH but including 6 M guanidine hydrochloride) were pipetted with a 16-channel 125 µL Viaflo pipette (Integra Biosciences) and Viaflo Assist (Integra Biosciences) (see Table S1 in Supplementary Data for the full dilution scheme). Finally, mixing was performed manually with new tips to minimize cross contamination between the wells. After mixing, the well plate was sealed with EASYseal™ sealing film (Steinheim, Germany) and incubated for 24 hours at room temperature. FLUOstar Omega microplate reader (BMG Labtech, Ortenberg, Germany) was used to measure the intrinsic fluorescence intensity of mAb1 at 330 and 350 nm after excitation at 280 nm. The measurements for both wavelengths were performed in multichromatic mode using 50 flashes per well and the same gain for each wavelength. The ratio between the fluorescence intensity at 350 and 330 nm (F350/330) was calculated for mAb1 in each denaturant concentration. The data from the triplicates was fitted to a three-state model and evaluated with the CDpal software [39]. Other models available in the software (e.g. two-state, three-state with dimerization of the intermediates, etc.) were also tested but showed poor fit quality in comparison to the three-state model we used. Different starting parameters for the C_m and m-values were tested and the different fits were compared with the f-test function of the software. The best fit was used to derive the values for C_m1, C_m2 and dG. The errors for the C_m and dG values are shown as

https://doi.org/10.1016/j.ejpb.2018.01.004

the Jackknife error from the fit. ddG was calculated such that the dG value for the lowest protein concentration was subtracted from the dG determined for the respective higher protein concentration.

2.4. pH measurements at different temperatures

The pH measurements were performed with an InLab Expert Pro-ISM pH electrode (Mettler Toledo, Germany) and a SevenEasy pH meter (Mettler Toledo, Germany). 10 mL of each buffer were filled in triplicates in 15 mL Falcon tubes. The Falcon tubes were immersed in water bath which temperature was increased in a step of 5 or 10 °C. After each increase, the samples were equilibrated for at least 5 minutes to reach constant temperature. Before measurement of the samples, the pH electrode was calibrated at each temperature with two calibration buffers pH 2 at 25 °C and pH 7 at 25 °C (Bernd Kraft, Germany) using the pH values provided from the manufacturer for the respective temperature.

2.5. Accelerated stability study and size exclusion chromatography (SEC)

mAb1 formulations with a concentration of 10 g/L were sterile filtered with 0.22 µm cellulose acetate filters from VWR International (Darmstadt, Germany). Next, 1 mL of each formulation was aseptically filled in sterilized type one glass vials (DIN 2R) and closed with sterilized rubber stoppers. The samples were incubated for 3 months at 40 ^{o}C ±2 ^{o}C. Every four weeks 50 µL were withdrawn from each replicate in a way that sterility of the solution is preserved. The samples were analyzed on a Waters Alliance 2690 separation module with a Waters 2487 UV/Vis detector and a Tosoh TSKgel G3000SWXL 7.8mm ID x 30.0 cm L column (Tokyo, Japan). The flow rate was 1 mL/min and the protein elution was detected at 280 nm after 25 µg protein were injected on the column. The mobile phase consisted of 25 mM sodium phosphate and 200 mM sodium chloride, the pH was adjusted to 7.0 ±0.05 with 2 M sodium hydroxide. The chromatograms were integrated with the Chromeleon 6.8 software (Thermo Fisher, Dreieich, Germany) and the relative percentage of high molecular weight (HMW) and low molecular weight (LMW) species was calculated to the total area of all protein peaks. As HMW are evaluated peaks eluting earlier than the monomer, while as LMW are evaluated protein peaks eluting later than the monomer. Next, the data was fitted linearly to obtain relative aggregation and fragmentation rates. The values for these rates and the corresponding adj. R^2 from the fits are provided (Table S2. in Supplementary Data).

3. Results and Discussion

3.1. Screen for optimal buffer and pH range

3.1.1. Unfolding and aggregation of mAb1 during thermal denaturation

mAb1 shows two unfolding transitions measured by the change of the intrinsic fluorescence ratio F350/330 in the temperature range 30 to 90 °C in all buffers we tested (Figure 1A and 1B). Previous work on mAbs shows that the first unfolding transition is assigned to the unfolding of the CH2 domain, while the second transition is assigned to the Fab and/or the CH3 domains [44]. Also, static light scattering at 473 nm showed that mAb1 aggregates in all conditions with the onset of the second unfolding transition but never during the first transition (Figure S1. in Supplementary Data).

3.1.2. Melting temperatures of mAb1 in various buffers

https://doi.org/10.1016/j.ejpb.2018.01.004

The melting temperatures of mAb1 across the pH range from 4.5 to 8.5 was investigated in four different buffers – 50 mM citrate pH 4.5 to 5.5, 50 mM phosphate pH 6 to 8.5, 50 mM histidine pH 5 to 6 and 50 mM tris pH 7.5 to 8.5 (Figure 2). The general trend shows a sharp decrease of both T_m1 and T_m2 with a decrease in pH below 6.0 in histidine and citrate. Also, both melting temperatures slightly decrease when the pH is increased above pH 6.5 in phosphate.

Highest T_m1 values were measured in 50 mM phosphate in the pH range 6.5 to 7 and in all tris formulations. Highest T_m2 values were measured in 50 mM citrate pH 5.5 and in 50 mM phosphate pH 6 and 7 as well as in tris formulations with pH 7.5 and 8 (at 25 °C). Interestingly, mAb1 showed lower T_m values in histidine compared to formulations with citrate or phosphate having the same pH at 25 °C. These differences were more distinct for the second melting temperature. On the other hand, mAb1 has in general higher T_m values in tris compared to phosphate in the pH range 7.5 to 8.5.

Similar observations with thermal denaturation studies of mAbs can be found in the literature. Razinkov et al. has reported that the melting temperatures of several mAbs measured by DSC and DSF were lower in histidine buffer in comparison to acetate or phosphate, indicating that "at pH 5.5, the mAbs were more stable in acetate buffer than in the histidine buffer" [13]. Menzen et al. used DSF with two different extrinsic fluorescent dyes to study the melting temperatures of a model mAb in various formulations [45]. They showed that the T_ms of the mAb were always lower in histidine pH 5 when compared to formulations with phosphate pH 5. This was true for a wide range of protein concentrations from 0.8 to 40 g/L. Interestingly, in the same work from Menzen et al. the melting temperatures of the same antibody were higher in histidine than in phosphate at pH 7.2. Another example is a recent work from Kalonia et. al where µDSC was used to evaluate the thermal stability of a model mAb and reported that "mAb in pH 4.5 and 6.5 citrate solutions had higher onset and melting temperatures compared to the mAb in histidine solution" [46].

Since histidine is a very common buffer for therapeutic proteins, especially for mAbs [37], an explanation with low physical stability of mAb1 in this buffer is unlikely. Therefore, we hypothesized that such disagreements between histidine and citrate or phosphate buffers might be due to change in buffer properties, more specifically due to buffer pH shift during heating and thermal denaturation experiments.

3.1.3. pH temperature dependence of the tested buffers

The pH of 50 mM citrate buffer pH 5 (at 20 °C) was measured over the temperature range 20 to 80 °C and compared to 50 mM histidine buffer pH 5 (at 20 °C) (Figure 3A). The pH of histidine decreases linearly and reaches 4.2 at 80 °C, while citrate exhibits a slight increase from pH 5.05 at 20 °C to pH 5.2 at 80 °C. Similar observations were made when we compared 50 mM phosphate buffer pH 6 (at 20 °C) with 50 mM histidine buffer pH 6 (at 20 °C) (Figure 3B). The slope of pH decrease (dpH/dT) for histidine was -0,014/1 °C and was the same for pH 5 and pH 6 formulations. The pH of citrate and phosphate remained almost unchanged over the investigated temperature range (i.e. dpH/dT was close to zero). This revealed that although having the same starting pH at 20 °C, when the buffers are heated to about 60-65 °C (the approximate temperature of T_m1 for mAb1) there is a difference of 0.7 pH units between citrate and histidine (Figure 3A) and a difference of 0.5 pH units between phosphate and histidine (Figure 3B). This difference becomes even bigger at temperatures around 80 °C (where approximately T_m2 of mAb1 is). Additionally, we also measured the dpH/dT for tris which was -0,022/1 °C for tris

https://doi.org/10.1016/j.ejpb.2018.01.004

buffers with pH 7.5, pH 8.0 and pH 8.5 at 20 ^{o}C, indicating that tris formulations will exhibit even larger pH shifts than histidine formulations during heating.

Considering the high pH dependence of the T_ms of mAb1 (Figure 2), especially at a pH below 6, such pH shifts during heating can significantly affect the melting temperatures of the measured protein. This can result in two possible scenarios. In the first case, the pH of the buffer is shifted away from the pH of maximum stability during heating and the T_m values appear lower. This is the case for the T_ms of mAb1 in histidine in Figure 2. In the second case, the pH is shifted towards the pH of maximum stability of the protein and the T_m values appear higher. This is the case for the T_ms of mAb1 in tris in Figure 2.

It is a well known fact that the behaviour of a certain buffer during heating will be determined mostly by its enthalpy of ionisation $dH_{ionisation}$ [47]. High positive or negative $dH_{ionisation}$ will indicate high temperature dependence of the acidic constant pKa, while ionisation enthalpy close to zero will indicate low temperature dependence of pKa. Subsequently, changes in pKa will influence the pH of the system according to the Henderson–Hasselbalch equation. A quick comparison between the $dH_{ionisation}$ and the dpH/dT shows that both values are in good agreement for the buffers we tested (for pK_2 of histidine $dH_{ionisation}$~ 30 kJ/mol, for tris $dH_{ionisation}$ ~47 kJ/mol; for pKa_2 and pKa_3 of citrate $dH_{ionisation}$ ~ 2 kJ/mol and ~-3 kJ/mol respectively; for pKa2 of phosphate $dH_{ionisation}$ ~4 kJ/mol [48]). Although, $dH_{ionisation}$ and dpKa/dT will indicate if a large dpH/dT can be expected, a good practice would be to measure the pH of each formulation for thermal denaturation in the temperature range of interest to determine the exact dpH/dT and avoid mistakes arising from comparison of formulations with different dpH/dT.

Even if the exact pH of a formulation buffer at a given temperature is known, corrections for the pH and melting temperatures should be done with great caution. The reason for this is that the temperature during thermal denaturation studies is increased relatively quickly (typically 0.5 - 1 ^{o}C/min) and this might not allow enough time for the protein to reach equilibrium state at the new pH before it unfolds. We assume that at the temperature and pH of unfolding the protein might be in a state that would not represent its "true" T_m value for a given formulation condition. Therefore, a direct comparison of the physical stability of a protein in buffers with different dpH/dT would be reliable only with suitable isothermal techniques.

3.1.4. Unfolding of mAb1 with isothermal chemical denaturation (ICD)

mAb1 shows a three-state unfolding transition after chemical denaturation with guanidine hydrochloride in all formulations tested (Figure 4). In another work with monoclonal antibody, the first transition was assigned to the unfolding of the CH2 domain while the second transition corresponds to the unfolding of the Fab and/or the CH3 domain [49]. This unfolding behaviour is also in good agreement with the unfolding curves during thermal denaturation. Direct comparison of the denaturation graphs (obtained with ICD) of mAb1 in histidine and citrate or in histidine and phosphate reveals that in most cases higher concentrations of guanidinium hydrochloride are needed to unfold the model mAb in histidine which is an indicator for higher physical stability of mAb1 in histidine.

The denaturation graphs of mAb1 in different formulations were evaluated with CDpal as described in the materials and methods section. An example fit of a sample denaturation graph can be found in the supplementary data (Figure S2). The C_m and dG values obtained from the best fit are used for further

comparison of the stability of the formulations. C_m1 was derived from the unfolding at lower denaturant concentration while C_m2 is derived from the unfolding at higher denaturant concentration.

3.1.4.1. C_m values of mAb1 in various buffers

As alkaline pH conditions (pH >7) are known to promote chemical degradation in mAb formulations and are thus not practically relevant, ICD and accelerated stability testing was limited to pH ranges 4.5-7 [21].

Both C_m1 and C_m2 of mAb1 show an increase with the increase of pH in all buffers (Figure 5) which is in a good agreement with the increase of T_m1 and T_m2 when the pH is increased from pH 4.5 to pH 6.5 (Figure 2). The C_m values of mAb1 in histidine are similar or higher than the C_m values in the citrate of phosphate formulations with the same pH, while the T_m1 and T_m2 values of mAb1 in histidine formulations were lower compared to their citrate and phosphate counterparts. One reason for this is that ICD is an isothermal technique and any pH temperature drift of excipients is avoided.

3.1.4.2. Concentration dependence of dG of mAb1 in various buffers

The Gibbs free energy of unfolding (dG) can be an indicator of protein conformational stability [32,40]. However, it has recently been demonstrated that dG is concentration dependent and this dependence can change in different formulations of the same protein [41]. Therefore, a comparison of different formulations based on a dG value determined at single protein concentration is rather difficult. On the other hand, the concentration dependence of dG is supposed to give indications whether a protein will be more aggregation prone in certain conditions [41]. High concentration dependence of dG indicates higher aggregation propensity of the protein while low concentration dependence of dG is an indicator for low aggregation propensity of the protein. To evaluate the feasibility of this approach, we investigated the concentration dependence of dG of mAb1 in the range of 0.5 to 4 g/L for several formulations. In our experiments, we observed that mAb1 shows the lowest concentration dependence (within ± 10 kJ/mol) of dG in citrate pH 5.0 and 5.5 (Figure 6A) and in histidine pH 6.0 (Figure 6B). The highest concentration dependence (more than ± 25 kJ/mol) of dG was observed in phosphate pH 6 and pH 6.5 (Figure 6C). This indicates that phosphate is a bad buffer choice for mAb1 despite the high T_m and C_m values of mAb1 measured in it.

3.1.5. Physical degradation of mAb1 in various buffers during accelerated stability studies

To validate the predictions made with thermal and chemical denaturation we performed accelerated stability studies for 12 weeks at 40 °C. We observed that not only aggregation but also fragmentation of mAb1 occurred in the samples we tested. Fragmentation was independent of the buffer we used (Figure 7B), but was highly dependent on the pH showing a minimum at pH 5.5 and 6 which is in a good agreement with previously published data for mAbs [21,50]. On the other hand, apparent aggregation rates were dependent not only on the pH but also on the buffer type (Figure 7A). Minimal aggregation rates of mAb1 were observed in all histidine formulations, followed by citrate formulations with pH 5.0 and 5.5. Highest aggregation rates of mAb1 were observed in phosphate pH 6.5 followed by

phosphate pH 7 and 6. At this point we should underline that the accelerated stability study in our case did not include analytical methods to evaluate chemical degradation (e.g. oxidation, deamination) and/or changes in the activity of the protein (both of which can be observed during storage). As already discussed in the introduction, such changes can also affect product quality and should be studied in parallel with the physical degradation.

3.1.6. Relationship between the physical stability indicating parameters and the aggregation rate at 40 °C

Both T_m and C_m values indicated that mAb1 should have high stability in phosphate buffer. Even worse, due to the pH shift of histidine, it appeared that the physical stability of mAb1 would be lower in histidine than in citrate or phosphate due to the lower T_m values of mAb1 measured in histidine. At this point, the only approach that indicated that phosphate is a bad buffer for mAb1 was the concentration dependence of dG. Also, all formulations with minimal concentration dependence of dG in Figure 6 showed very low apparent aggregation rate (Figure 7A), but not vice versa. Still, if the formulations with minimal concentration dependence of dG were selected, this would have resulted in satisfactory results in the accelerated stability studies in this case. However, we should note that the approach to determine the concentration dependence of dG requires more sample in comparison to high throughput methods like DSF.

3.1.7. Rational use of a combination from DSF and ICD to study protein physical stability in different formulations

Based on our work, we suggest that a *combination of DSF and ICD* would be feasible to reduce the protein amount required to assess the physical stability in various formulations but still provide sufficient prediction quality. Such a combination would:

- *First - Employ DSF to study the melting temperatures of a new therapeutic protein candidate over a wide pH range in buffers with dpH/dT close to zero to determine the pH range of maximum T_m values;*
- *Second – Use ICD to determine C_m, dG and the concentration dependence of dG of the therapeutic protein candidate in the pH range of maximum T_m values in various buffers (which can have high dpH/dT e.g. histidine, tris);*
- *Third – Perform accelerated stability tests on formulations with the highest T_m, highest C_m and lowest concentration dependence of dG.*

3.2. Final words and recommendations

High throughput thermal denaturation is a valuable technique to determine the melting temperatures of therapeutic protein candidates in early stage development when the amount of material available is limited. When it comes to formulation studies, thermal denaturation techniques in general are (alongside other pitfalls discussed in the introduction) limited by the fact that increase in temperature can change key properties of the excipients (i.e. pH of the buffer system). Care should be taken when such measurements are conducted. pH screenings based on T_m values should be performed only in buffers with dpH/dT close to zero. After the pH range of maximum thermal stability of a protein is found, further formulation experiments with a wider range of buffers should be performed with isothermal techniques. A suitable isothermal technique that can be used at this stage is isothermal chemical denaturation. ICD would allow direct comparison of a variety of formulations buffers regardless of their dpH/dT. Moreover, investigation of the concentration dependence of dG is a

valuable tool which can allow identification of “bad” conditions where the protein has low physical stability during storage.

4. Acknowledgements

This study was funded by a project part of the EU Horizon 2020 Research and Innovation programme under the Marie Skłodowska-Curie grant agreement No 675074. The authors would also like to thank the Erasmus+ Traineeship programme for funding the research stay of U.M in Munich. Moritz Schroll is acknowledged for performing the pH measurements of buffers at different temperatures.

5. References

[1] D.S. Dimitrov, Therapeutic Proteins, in: V. Voynov, J.A. Caravella (Eds.), Ther. Proteins Methods Protoc., Humana Press, Totowa, NJ, (2012) 1–26. doi:10.1007/978-1-61779-921-1_1.

[2] D.S. Dimitrov, Therapeutic antibodies, vaccines and antibodyomes, MAbs. 2 (2010) 347–356. doi:10.4161/mabs.2.3.11779.

[3] J.G. Elvin, R.G. Couston, C.F. Van Der Walle, Therapeutic antibodies: Market considerations, disease targets and bioprocessing, Int. J. Pharm. 440 (2013) 83–98. doi:10.1016/j.ijpharm.2011.12.039.

[4] L. DeFrancesco, Drug pipeline Q4 2015, Nat Biotech. 34 (2016) 128. http://dx.doi.org/10.1038/nbt.3484.

[5] W. Wang, D.N. Kelner, Correlation of rFVIII inactivation with aggregation in solution, Pharm. Res. 20 (2003) 693–700. doi:10.1023/A:1023271405005.

[6] L. Runkel, W. Meier, R.B. Pepinsky, M. Karpusas, A. Whitty, K. Kimball, M. Brickelmaier, C. Muldowney, W. Jones, S.E. Goelz, Structural and Functional Differences Between Glycosylated and Non-glycosylated Forms of Human Interferon-$β$ (IFN-$β$), Pharm. Res. 15 (1998) 641–649. doi:10.1023/A:1011974512425.

[7] E.M. Moussa, J.P. Panchal, B.S. Moorthy, J.S. Blum, M.K. Joubert, L.O. Narhi, E.M. Topp, Immunogenicity of Therapeutic Protein Aggregates, J. Pharm. Sci. 105 (2017) 417–430. doi:10.1016/j.xphs.2015.11.002.

[8] S. Sethu, K. Govindappa, M. Alhaidari, M. Pirmohamed, K. Park, J. Sathish, Immunogenicity to Biologics: Mechanisms, Prediction and Reduction, Arch. Immunol. Ther. Exp. (Warsz). 60 (2012) 331–344. doi:10.1007/s00005-012-0189-7.

[9] K.D. Ratanji, J.P. Derrick, R.J. Dearman, I. Kimber, Immunogenicity of therapeutic proteins: Influence of aggregation, J. Immunotoxicol. 11 (2014) 99–109. doi:10.3109/1547691X.2013.821564.

[10] C. ICH, Q 6 B Specifications: Test Procedures and Acceptance Criteria for Biotechnological/Biological Products, Eur. Med. Agency. (1999) 1–17.

[11] A. Hawe, M. Wiggenhorn, M. van de Weert, J.H.O. Garbe, H. Mahler, W. Jiskoot, Forced degradation of therapeutic proteins, J. Pharm. Sci. 101 (2012) 895–913. doi:10.1002/jps.22812.

[12] M.A.H. Capelle, R. Gurny, T. Arvinte, High throughput screening of protein formulation

stability: Practical considerations, Eur. J. Pharm. Biopharm. 65 (2007) 131–148. doi:10.1016/j.ejpb.2006.09.009.

[13] F. He, S. Hogan, R.F. Latypov, L.O. Narhi, V.I. Razinkov, High throughput thermostability screening of monoclonal antibody formulations, J. Pharm. Sci. 99 (2010) 1707–1720. doi:10.1002/jps.21955.

[14] D.S. Goldberg, S.M. Bishop, A.U. Shah, H.A. Sathish, Formulation development of therapeutic monoclonal antibodies using high-throughput fluorescence and static light scattering techniques: Role of conformational and colloidal stability, J. Pharm. Sci. 100 (2011) 1306–1315. doi:10.1002/jps.22371.

[15] D.S. Goldberg, R. Lewus, R. Esfandiary, D. Farkas, N. Mody, K. Day, P. Mallik, M.B. Tracka, S.K. Sealey, H.S. Samra, Utility of High Throughput Screening Techniques to Predict Stability of Monoclonal Antibody Formulations During Early Stage Development, J. Pharm. Sci. 106 (2017) 1971-1977. doi:10.1016/j.xphs.2017.04.039.

[16] R. Chaudhuri, Y. Cheng, C.R. Middaugh, D.B. Volkin, High-Throughput Biophysical Analysis of Protein Therapeutics to Examine Interrelationships Between Aggregate Formation and Conformational Stability, AAPS J. 16 (2014) 48–64. doi:10.1208/s12248-013-9539-6.

[17] N.R. Maddux, V. Iyer, W. Cheng, A.M.K. Youssef, S.B. Joshi, D.B. Volkin, J.P. Ralston, G. Winter, C. Russell Middaugh, High throughput prediction of the long-term stability of pharmaceutical macromolecules from short-term multi-instrument spectroscopic data, J. Pharm. Sci. 103 (2014) 828–839. doi:10.1002/jps.23849.

[18] C.J. Roberts, Therapeutic protein aggregation: mechanisms, design, and control, Trends Biotechnol. 32 (2014) 372–380. doi:http://dx.doi.org/10.1016/j.tibtech.2014.05.005.

[19] E.Y. Chi, S. Krishnan, T.W. Randolph, J.F. Carpenter, Physical Stability of Proteins in Aqueous Solution: Mechanism and Driving Forces in Nonnative Protein Aggregation, 20 (2003) 1325 - 1336. https://doi.org/10.1023/A:1025771421906

[20] W. Wang, S. Nema, D. Teagarden, Protein aggregation-Pathways and influencing factors, Int. J. Pharm. 390 (2010) 89–99. doi:10.1016/j.ijpharm.2010.02.025.

[21] M.C. Manning, D.K. Chou, B.M. Murphy, R.W. Payne, D.S. Katayama, Stability of protein pharmaceuticals: An update, Pharm. Res. 27 (2010) 544–575. doi:10.1007/s11095-009-0045-6.

[22] C.M. Johnson, Differential scanning calorimetry as a tool for protein folding and stability, Arch. Biochem. Biophys. 531 (2013) 100–109. doi:http://dx.doi.org/10.1016/j.abb.2012.09.008.

[23] L. Burton, R. Gandhi, G. Duke, M. Paborji, Use of Microcalorimetry and Its Correlation with Size Exclusion Chromatography for Rapid Screening of the Physical Stability of Large Pharmaceutical Proteins in Solution, Pharm. Dev. Technol. 12 (2007) 265–273. doi:10.1080/10837450701212610.

[24] M.L. Brader, T. Estey, S. Bai, R.W. Alston, K.K. Lucas, S. Lantz, P. Landsman, K.M. Maloney, Examination of thermal unfolding and aggregation profiles of a series of developable therapeutic monoclonal antibodies, Mol. Pharm. 12 (2015) 1005–1017. doi:10.1021/mp400666b.

[25] V. Kumar, N. Dixit, L. Zhou, W. Fraunhofer, Impact of short range hydrophobic interactions and long range electrostatic forces on the aggregation kinetics of a monoclonal antibody and a dual-variable domain immunoglobulin at low and high concentrations, Int. J. Pharm. 421

(2011) 82–93. doi:10.1016/j.ijpharm.2011.09.017.

[26] A.M.K. Youssef, G. Winter, A critical evaluation of microcalorimetry as a predictive tool for long term stability of liquid protein formulations: Granulocyte Colony Stimulating Factor (GCSF), Eur. J. Pharm. Biopharm. 84 (2013) 145–155. doi:10.1016/j.ejpb.2012.12.017.

[27] U.B. Ericsson, B.M. Hallberg, G.T. DeTitta, N. Dekker, P. Nordlund, Thermofluor-based high-throughput stability optimization of proteins for structural studies, Anal. Biochem. 357 (2006) 289–298. doi:http://dx.doi.org/10.1016/j.ab.2006.07.027.

[28] R. Wanner, D. Breitsprecher, S. Duhr, P. Baaske, G. Winter, Thermo-Optical Protein Characterization for Straightforward Preformulation Development, J. Pharm. Sci. 106 (2017) 2955–2958. http://dx.doi.org/10.1016/j.xphs.2017.06.002

[29] T.A. Menzen, Temperature-Induced Unfolding, Aggregation, and Interaction of Therapeutic Monoclonal Antibodies, (2014). PhD thesis. LMU Munich. urn:nbn:de:bvb:19-175200

[30] A.C. King, M. Woods, W. Liu, Z. Lu, D. Gill, M.R.H. Krebs, High-throughput measurement, correlation analysis, and machine-learning predictions for pH and thermal stabilities of Pfizer-generated antibodies, Protein Sci. 20 (2011) 1546–1557. doi:10.1002/pro.680.

[31] D. Breitsprecher, N. Glücklich, A. Hawe, T. Menzen, Thermal Unfolding of Antibodies Comparison of nanoDSF and µDSC for thermal stability assessment during biopharmaceutical formulation development, Appl. Note. NT-PR-006 (2016).

[32] E. Freire, A. Schön, B.M. Hutchins, R.K. Brown, Chemical denaturation as a tool in the formulation optimization of biologics, Drug Discov. Today. 18 (2013) 1007–1013. doi:10.1016/j.drudis.2013.06.005.

[33] J.M. Sanchez-Ruiz, Theoretical analysis of Lumry-Eyring models in differential scanning calorimetry, Biophys. J. 61 (1992) 921–935. doi:10.1016/S0006-3495(92)81899-4.

[34] C.J. Roberts, T.K. Das, E. Sahin, Predicting solution aggregation rates for therapeutic proteins: Approaches and challenges, Int. J. Pharm. 418 (2011) 318–333. doi:10.1016/j.ijpharm.2011.03.064.

[35] H. Nagai, K. Kuwabara, G. Carta, Temperature dependence of the dissociation constants of several amino acids, J. Chem. Eng. Data. 53 (2008) 619–627. doi:10.1021/je700067a.

[36] J.C. Reijenga, L.G. Gagliardi, E. Kenndler, Temperature dependence of acidity constants, a tool to affect separation selectivity in capillary electrophoresis, J. Chromatogr. A. 1155 (2007) 142–145. doi:10.1016/j.chroma.2006.09.084.

[37] T.J. Zbacnik, R.E. Holcomb, D.S. Katayama, B.M. Murphy, R.W. Payne, R.C. Coccaro, G.J. Evans, J.E. Matsuura, C.S. Henry, M.C. Manning, Role of Buffers in Protein Formulations, J. Pharm. Sci. 106 (2017) 713–733. doi:10.1016/j.xphs.2016.11.014.

[38] C.N. Pace, K.L. Shaw, Linear extrapolation method of analyzing solvent denaturation curves., Proteins. Suppl 4 (2000) 1–7. doi:10.1002/1097-0134(2000)41:4+<1::AID-PROT10>3.0.CO;2-2 [pii].

[39] M. Niklasson, C. Andresen, S. Helander, M.G.L. Roth, A. Zimdahl Kahlin, M. Lindqvist Appell, L.-G. Mårtensson, P. Lundström, Robust and convenient analysis of protein thermal and chemical stability, Protein Sci. 24 (2015) 2055–2062. doi:10.1002/pro.2809.

[40] K.L. Lazar, T.W. Patapoff, V.K. Sharma, Cold denaturation of monoclonal antibodies, MAbs. 2

(2010) 42–52. doi:10.4161/mabs.2.1.10787.

[41] A. Schön, B.R. Clarkson, R. Siles, P. Ross, R.K. Brown, E. Freire, Denatured state aggregation parameters derived from concentration dependence of protein stability, Anal. Biochem. 488 (2015) 45–50. doi:10.1016/j.ab.2015.07.013.

[42] B.R. Clarkson, A. Sch??n, E. Freire, Conformational stability and self-association equilibrium in biologics, Drug Discov. Today. 21 (2016) 342–347. doi:10.1016/j.drudis.2015.11.007.

[43] J.M. Rizzo, S. Shi, Y. Li, A. Semple, J.J. Esposito, S. Yu, D. Richardson, V. Antochshuk, M. Shameem, Application of a high-throughput relative chemical stability assay to screen therapeutic protein formulations by assessment of conformational stability and correlation to aggregation propensity, J. Pharm. Sci. 104 (2015) 1632–1640. doi:10.1002/jps.24408.

[44] T. Menzen, W. Friess, Temperature-Ramped Studies on the Aggregation , Unfolding , and Interaction of a Therapeutic Monoclonal Antibody, J. Pharm. Sci. 103 (2014) 445–455. doi:10.1002/jps.23827.

[45] F. Menzen, Tim, Wolfgang, High-Throughput Melting-Temperature Analysis of a Monoclonal Antibody by Differential Scanning Fluorimetry in the Presence of Surfactants, J. Pharm. Sci. 102 (2013) 415–428. doi:10.1002/jps.23405

[46] C. Kalonia, V. Toprani, R. Toth, N. Wahome, I. Gabel, C.R. Middaugh, D.B. Volkin, Effects of Protein Conformation, Apparent Solubility, and Protein-Protein Interactions on the Rates and Mechanisms of Aggregation for an IgG1Monoclonal Antibody, J. Phys. Chem. B. 120 (2016) 7062–7075. doi:10.1021/acs.jpcb.6b03878.

[47] H. Fukada, K. Takahashi, Enthalpy and heat capacity changes for the proton dissociation of various buffer components in 0.1 M potassium chloride, Proteins Struct. Funct. Genet. 33 (1998) 159–166. doi:10.1002/(SICI)1097-0134(19981101)33:2<159::AID-PROT2>3.0.CO;2-E.

[48] R.N. Goldberg, N. Kishore, R.M. Lennen, Thermodynamic quantities for the ionization reaction of buffers., J. Phys. Chem. Ref. Data. 31 (2002) 231–370.

[49] H. Liu, C. Chumsae, G. Gaza-Bulseco, E.R. Goedken, Domain-level stability of an antibody monitored by reduction, differential alkylation, and mass spectrometry analysis, Anal. Biochem. 400 (2010) 244–250. doi:10.1016/j.ab.2010.02.004.

[50] J. Vlasak, R. Ionescu, Fragmentation of monoclonal antibodies Fragmentation of monoclonal antibodies, mAbs 3 , 862 (2017). doi:10.4161/mabs.3.3.15608.

Figure 1. *Thermal unfolding of mAb1 detected by intrinsic fluorescence ratio (F350/330) at: (A) pH 5 in 50 mM citrate (black) and 50 mM histidine (gray); (B) pH 6 in 50 mM phosphate (black) and 50 mM histidine (gray). An overlay of three separate measurements is given for each sample. The place where the T_m values are obtained from the first derivative are marked with a cross.*

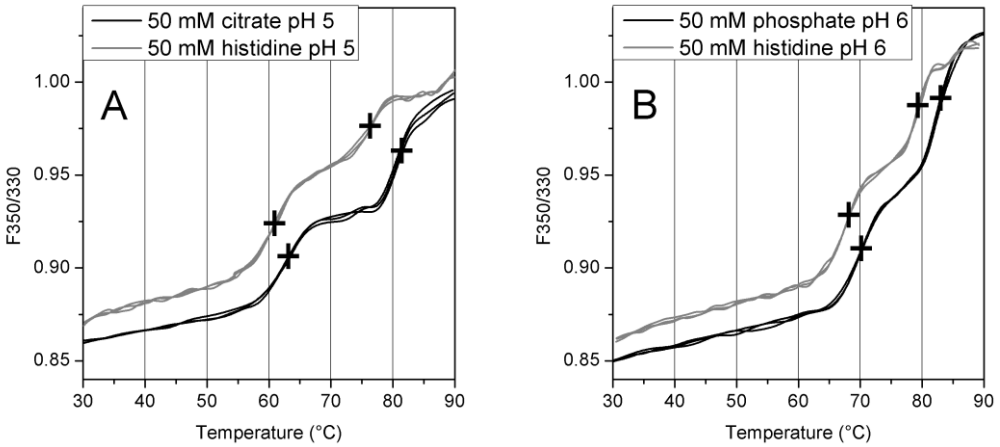

Figure 2. *Melting temperatures T_m1 (filled symbols) and T_m2 (open symbols) of mAb1 in different buffers measured with thermal denaturation and intrinsic fluorescence - 50 mM citrate (squares), 50 mM phosphate (circles), 50 mM histidine (triangles), 50 mM tris (diamonds). The pH shown on the graph is measured at 25 °C. The provided values are mean of three measurements and the error is the standard deviation.*

https://doi.org/10.1016/j.ejpb.2018.01.004

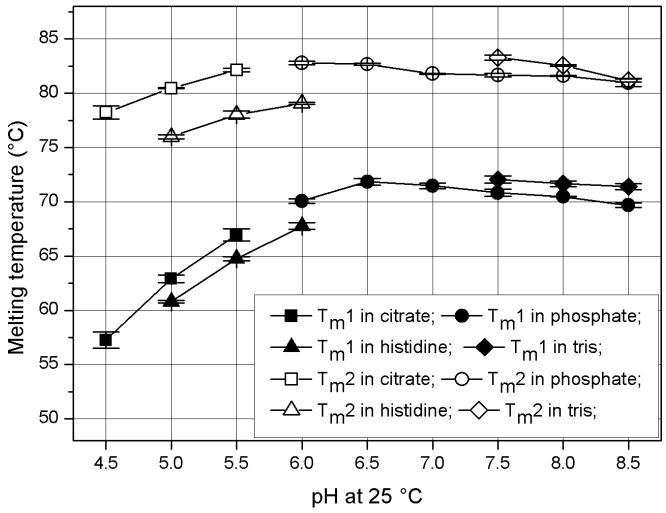

Figure 3. A. *pH of 50 mM citrate (squares) and 50 mM histidine (triangles) between 20 and 80 °C, both buffers had pH 5 at 20 °C;* ***B.*** *pH of 50 mM phosphate (circles) and 50 mM histidine (triangles) between 20 and 80 °C, both buffers had pH 6 at 20 °C; The values are mean of triplicates. The measurements were performed in triplicates and the deviations between the replicates were lower than 0.02 pH units.*

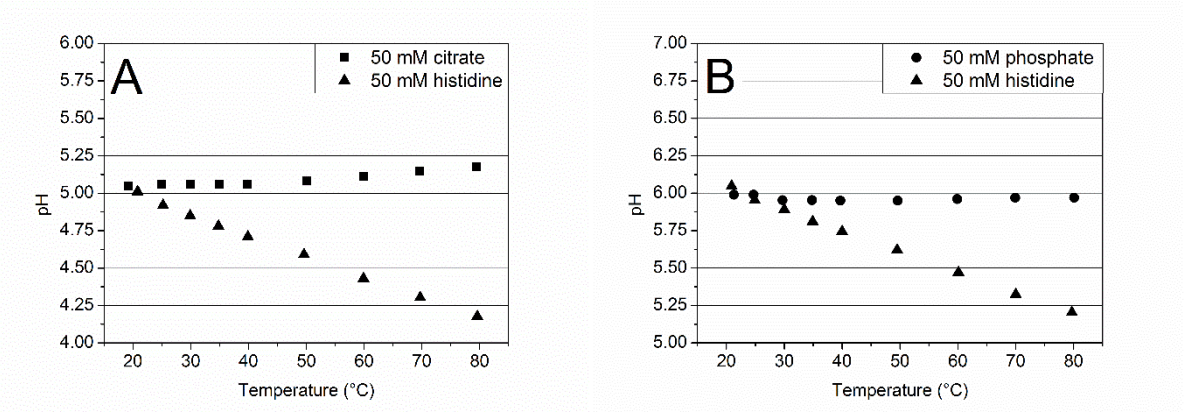

Figure 4. *Chemical denaturation of mAb1 detected by intrinsic fluorescence ratio (F350/330) at: (A) pH 5 in 50 mM citrate (squares) and 50 mM histidine (triangles); (B) pH 6 in 50 mM phosphate (circles) and 50 mM histidine (triangles). The lines on this graph are to guide the eyes and do not represent a fit to a certain model.*

https://doi.org/10.1016/j.ejpb.2018.01.004

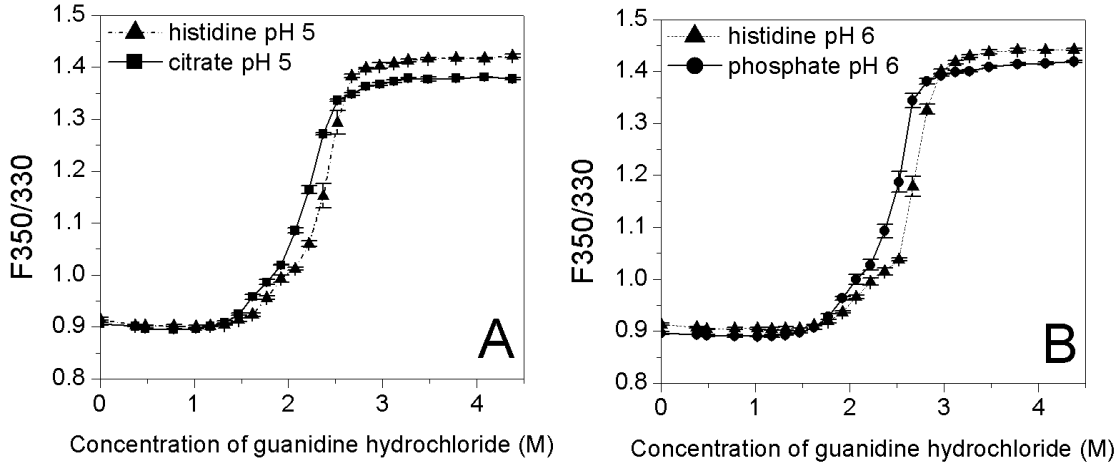

Figure 5. *C_m values - C_m1 (filled symbols) and C_m2 (open symbols) - of mAb1 in different buffers measured with chemical denaturation and intrinsic fluorescence - 50 mM citrate (squares), 50 mM phosphate (circles), 50 mM histidine (triangles). The pH of the shown on the graph is measured at 25 °C. The values are obtained from the fit of three denaturation graphs. The error bar represents the Jackknife error from the fit in CDpal.*

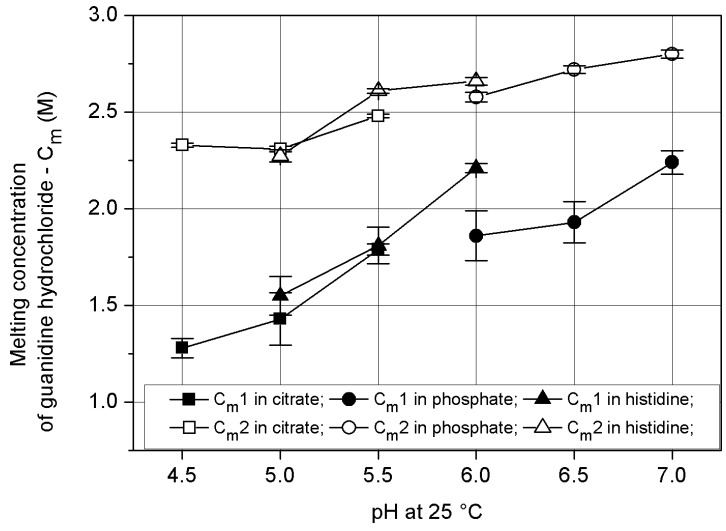

https://doi.org/10.1016/j.ejpb.2018.01.004

Figure 6. *Concentration dependence of dG for mAb1 in various buffers. A. 50 mM citrate with pH 4.5 (squares), pH 5 (circles) and 5.5 (triangles up); B. 50 mM histidine with pH 5 (squares), 5.5 (circles) and 6.0 (triangles up); C. 50 mM phosphate with pH 6 (triangles down), 6.5 (triangles left) and 7.0 (triangles right). Each point on the graphs is derived from three chemical denaturation graphs. The errors are the Jackknife error from the fit to the three-state mode in CDpal.*

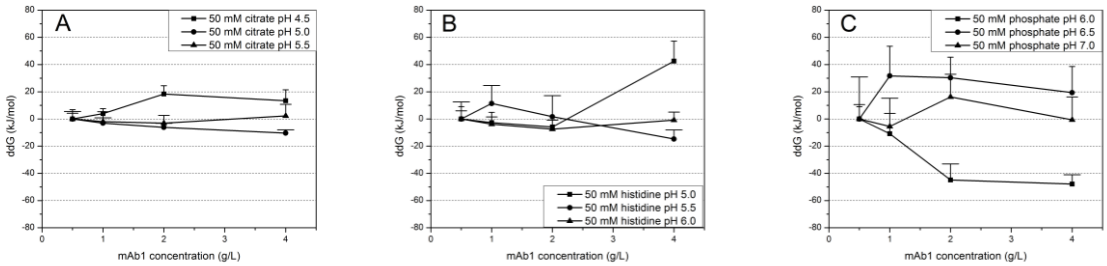

Figure 7. *A. Apparent aggregation rates of mAb1 in various buffers determined after 12-week storage at 40 °C; B. Apparent fragmentation rates of mAb1 in various buffers determined after 12-week storage at 40 °C;*

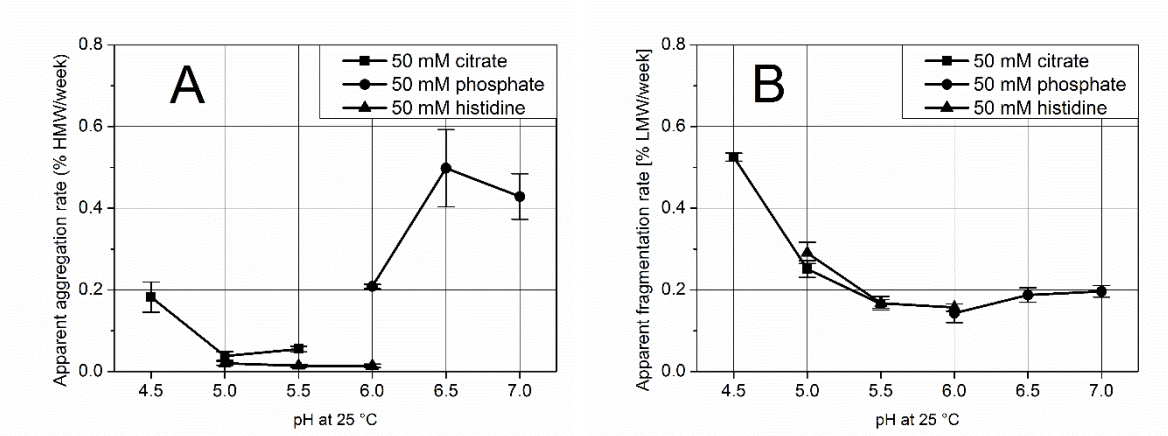

https://doi.org/10.1016/j.ejpb.2018.01.004

Supplementary Data

Table S1. Dilution scheme for isothermal chemical denaturation experiments

Row	Protein, µL	Buffer, µL	Denaturant, µL
1	8	72	0
2	8	67	5
3	8	65.6	6.4
4	8	61.6	10.4
5	8	58.4	13.6
6	8	56.4	15.6
7	8	54.4	17.6
8	8	52.4	19.6
9	8	50.4	21.6
10	8	48.4	23.6
11	8	46.4	25.6
12	8	44.4	27.6
13	8	42.4	29.6
14	8	40.4	31.6
15	8	38.4	33.6
16	8	36.4	35.6
17	8	34.4	37.6
18	8	32.4	39.6
19	8	30.4	41.6
20	8	28.4	43.6
21	8	25.6	46.4
22	8	21.6	50.4
23	8	17.6	54.4
24	8	13.6	58.4

Figure S1. Change in intrinsic fluorescence (F350/330) and static light scattering signal at 473 nm during thermal denaturation of mAb1 in 50 mM phosphate pH 6. High increase in the scattering is observed with the onset of the second unfolding transition.

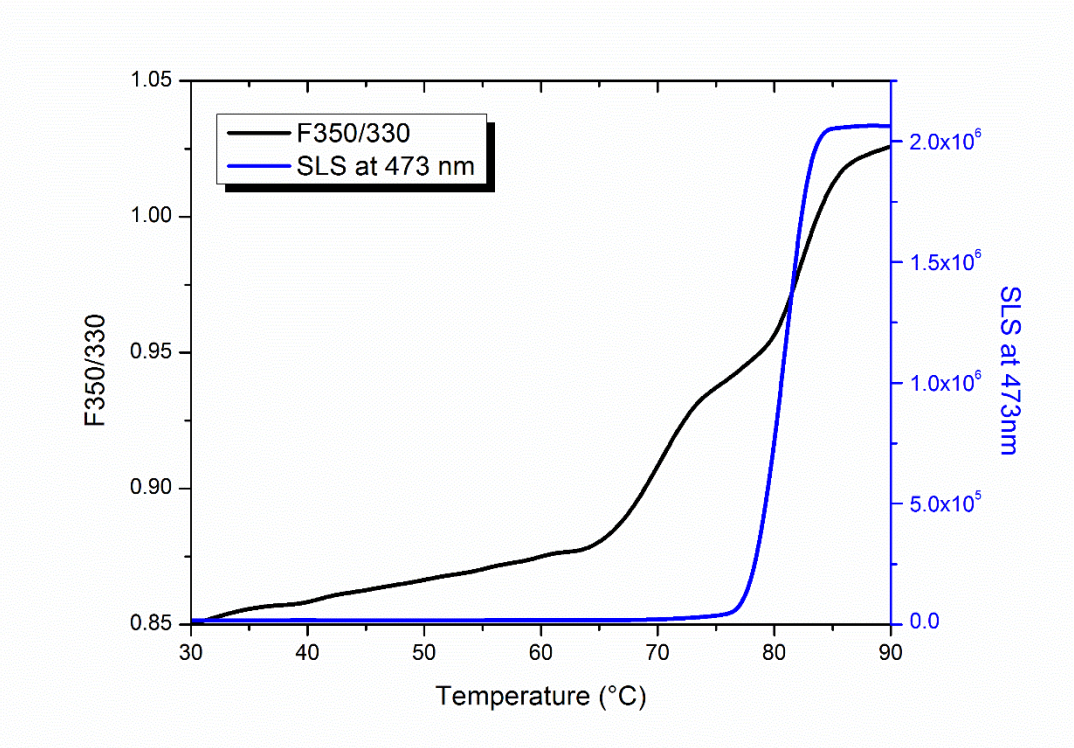

https://doi.org/10.1016/j.ejpb.2018.01.004

Figure S2. Example fit of chemical denaturation graph in CDpal

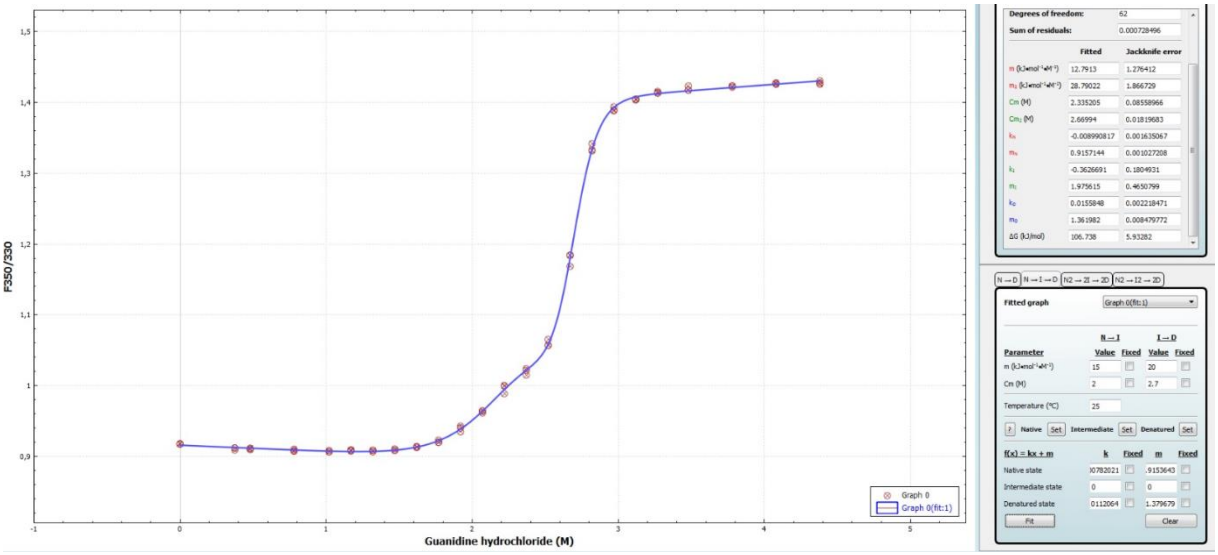

Figure S3. Chromatogram of mAb1 sample from Size Exclusion Chromatography. Integration of the HMW area was done from 5 to 8 minutes elution time. Integration for the LMW area was done from 10,5 to 12 minutes elution time.

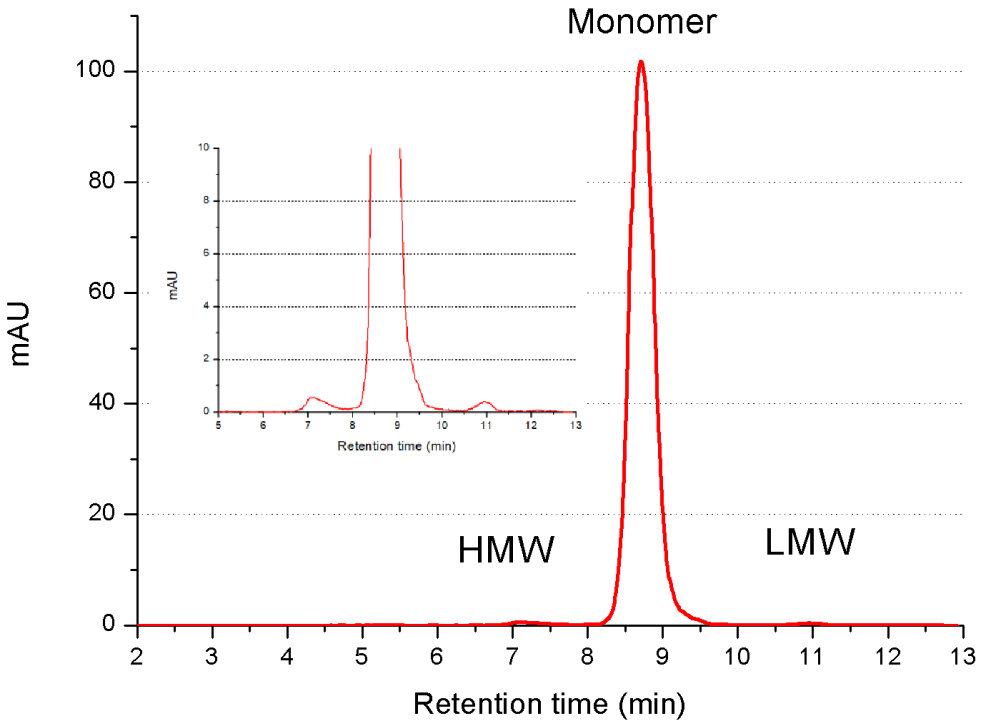

https://doi.org/10.1016/j.ejpb.2018.01.004

Table S2. Rate of HMW and LMW formation derived from linear fit of the data in Origin 8.0 with the corresponding adjusted R^2 values. The adjusted R^2 values are used as this is a parameter which describes the quality of the regression better than R^2. The adj. R^2 values are always lower than the corresponding R^2 values.

Buffer	50 mM citrate			50 mM phosphate			50 mM histidine		
pH	4,5	5,0	5,5	6,0	6,5	7,0	5,0	5,5	6,0
Rate of HMW formation (%/week)	0.18233	0.03808	0.05508	0.20833	0.49792	0.42883	0.02008	0.01425	0.0141
Error from the fit	0.03717	0.01078	0.00691	0.00553	0.09453	0.05566	0.00517	0.0039	0.00422
Adj. R^2	0.8849	0.79273	0.95429	0.99789	0.89914	0.9511	0.82454	0.80482	0.77425
Rate of LMW formation (%/week)	0.52508	0.251	0.16558	0.14308	0.1875	0.19633	0.29067	0.16733	0.157
Error from the fit	0.00976	0.02056	0.01085	0.02287	0.01767	0.01386	0.02596	0.01682	0.00914
Adj. R^2	0.99896	0.98014	0.98724	0.92708	0.97382	0.98519	0.97645	0.97029	0.9899

https://doi.org/10.1016/j.ejpb.2018.01.004